Jet-induced star formation in gas-rich galaxies

V. Gaibler,[1,2]★ S. Khochfar,[2] M. Krause[2,3] and J. Silk[4,5]

[1] *Institut für Theoretische Astrophysik, Zentrum für Astronomie der Universität Heidelberg, Albert-Ueberle-Str. 2, 69120 Heidelberg, Germany*
[2] *Max-Planck-Institut für Extraterrestrische Physik, Gießenbachstraße, 85748 Garching, Germany*
[3] *Excellence Cluster Universe, Technische Universität München, Boltzmannstraße 2, 85748 Garching, Germany*
[4] *Institut d'Astrophysique, 98 bis Boulevard Arago, 75014 Paris, France*
[5] *Department of Physics and Astronomy, Homewood Campus, The Johns Hopkins University, Baltimore, MD 21218, USA*

ABSTRACT

Feedback from active galactic nuclei (AGN) has become a major component in simulations of galaxy evolution, in particular for massive galaxies. AGN jets have been shown to provide a large amount of energy and are capable of quenching cooling flows. Their impact on the host galaxy, however, is still not understood. Subgrid models of AGN activity in a galaxy evolution context so far have been mostly focused on the quenching of star formation. To shed more light on the actual physics of the 'radio mode' part of AGN activity, we have performed simulations of the interaction of a powerful AGN jet with the massive gaseous disc (10^{11} M$_\odot$) of a high-redshift galaxy. We spatially resolve both the jet and the clumpy, multi-phase interstellar medium (ISM) and include an explicit star formation model in the simulation. Following the system over more than 10^7 yr, we find that the jet activity excavates the central region, but overall causes a significant change to the shape of the density probability distribution function and hence the star formation rate due to the formation of a blast wave with strong compression and cooling in the ISM. This results in a ring- or disc-shaped population of young stars. At later times, the increase in star formation rate also occurs in the disc regions further out since the jet cocoon pressurizes the ISM. The total mass of the additionally formed stars may be up to 10^{10} M$_\odot$ for one duty cycle. We discuss the details of this jet-induced star formation (positive feedback) and its potential consequences for galaxy evolution and observable signatures.

Key words: hydrodynamics – methods: numerical – ISM: clouds – galaxies: jets – galaxies: ISM – galaxies: star formation.

1 INTRODUCTION

Large scale cosmological simulations often include active galactic nuclei (AGN) feedback in massive galaxies in order to avoid both further growth of massive galaxies via star formation and the presence of a young stellar population at low redshift (e.g. Bower et al. 2006; Croton et al. 2006; Hopkins et al. 2006; Schawinski et al. 2006). This approach is quite natural since AGN activity is frequently observed in these galaxies (Best et al. 2005). So far, the models focus on negative feedback (suppression of star formation) to quench cooling flows, remove potentially star-forming gas by expelling it from the galaxy or heating the interstellar gas to high temperatures in the halo to prevent new stars from forming. In contrast to radiation-based 'quasar mode' feedback at high accretion rates, 'radio mode' feedback by jets is powered mechanically by the kinetic energy of the jet beam (Blandford & Rees 1974;

Scheuer 1974). For the case of cooling flows in clusters of galaxies and giant ellipticals, there is also meanwhile considerable evidence from observations of X-ray cavities that the energies deposited by the jets suffice in many cases to suppress the formation of cooling flows in the hot circum-galactic and intra-cluster media (e.g. Bîrzan et al. 2004; Dunn, Fabian & Taylor 2005; Rafferty et al. 2006). Furthermore, theoretical studies (e.g. Zanni et al. 2005; Gaibler, Krause & Camenzind 2009; O'Neill & Jones 2010) show a high thermalization efficiency for this interaction.

In this paper, we examine the impact of jet feedback on the star formation in massive, gas-rich galaxies at high redshift ($z \sim 2$–3). It is not obvious why jet feedback, which acts in a negative manner on the hot and dilute circum-galactic X-ray gas, should also act similarly on the interstellar medium (ISM), since this is a multi-phase medium with much higher densities and a pronounced clumpy density structure in dynamic equilibrium between gas at various densities and temperatures (de Avillez & Breitschwerdt 2005). An alternative option is the model of positive feedback, where jet activity actually triggers or enhances star formation in

★E-mail: v.gaibler@uni-heidelberg.de

a galaxy (Silk 2005). This is, however, generally applied on the galaxy scales and without explicit hydrodynamical modelling in large-scale cosmological simulations.

Observational studies on this issue so far are inconclusive. Locally, one-third of the radio galaxies show bright emission from warm molecular gas and very low to moderate star formation rates (SFRs) (Ogle et al. 2007, 2010; Nesvadba et al. 2010). The jets seem to heat the cold molecular gas and keep it warm during the lifetime of the jet although the cooling times are much shorter than the jet lifetime – potentially due to the action of shocks, turbulent dissipation or cosmic rays (Ferland et al. 2008, 2009; Guillard et al. 2009; Papadopoulos et al. 2010). The jets in those sources may actually induce formation of molecular gas but not cause the formation of a detectable number of stars (Nesvadba et al. 2011). Shock-heated, dense and turbulent gas has also been predicted in multi-phase turbulence simulations for jet cocoons (Krause & Alexander 2007). Positive feedback, on the other hand, is directly supported by only a few observations locally (Minkowski's object in Croft et al. 2006, Centaurus A in Mould et al. 2000; Morganti 2010), at intermediate (PKS2250-41 in Inskip et al. 2008) and high redshift (4C 41.17 in Dey et al. 1997; Bicknell et al. 2000). But several studies point towards a link between jets and star formation, such as a high incidence of recent star formation activity in compact radio sources (Dicken et al. 2012), the detection of large masses of cold molecular gas in high redshift radio galaxies (e.g. Emonts et al. 2011), alignment of excited CO with jets (Klamer et al. 2004), alignment of continuum emission (Chambers, Miley & van Breugel 1987; McCarthy et al. 1987) and a correlation of emission line gas (McCarthy, van Breugel & Kapahi 1991) with the radio source. Furthermore, several authors find evidence for young stellar populations in radio galaxies (Tadhunter et al. 2002; Wills et al. 2002; Baldi & Capetti 2008; Tadhunter et al. 2011) and their central regions (Aretxaga et al. 2001), possibly accounting for a substantial mass fraction (Holt et al. 2007). It is important to keep in mind that the circumstances of jet feedback vary largely throughout these studies since gas masses and the velocity dispersions are much larger at high redshift (a setting that we are addressing in this paper) than in the local Universe, and variations amongst radio galaxies of a certain redshift regime are also large.

We are still in an early stage of understanding jet feedback, despite very detailed observational studies in this field. The lack of physical modelling and understanding of jet feedback is currently one of the major shortcomings of 'radio mode' feedback scenarios on galaxy scales. Only recently, high resolution hydrodynamical simulations including a clumpy ISM have become feasible (Sutherland & Bicknell 2007; Gaibler, Khochfar & Krause 2011; Wagner & Bicknell 2011). Indeed, these studies have shown that the multi-phase structure of the ISM causes the morphology and jet–gas interaction to be qualitatively different from simulations without the cooler and denser phases. Antonuccio-Delogu & Silk (2008) and Tortora et al. (2009) have studied the interaction of a powerful jet in 2D slab geometry with cool clumps of gas dispersed within a hot medium, finding only a slight increase in the star formation (10–20 per cent) followed by a much stronger decrease (more than 50 per cent) within a few million years due to heating and ablation of the cloud gas. However, the 2D approach results in a different pressure evolution of the cocoon and a larger effective surface of the clouds than in 3D. Wagner & Bicknell (2011) studied the interaction of a relativistic jet with a clumpy gas distribution in a galaxy's centre at high resolution. They found a considerable impact of the filling factor of the dense gas on the interaction efficiency and that the dispersal of gas at large velocities may actually inhibit star formation. Yet, their

simulated time-scales of $\lesssim 1$ Myr allow only a weak impact of cooling and the simulations do not explicitly include a star formation model.

In our previous paper (Gaibler et al. 2011, hereafter Paper I), we found that the action of jets in a clumpy medium results in a complex interaction with both individual clumps and the average density distribution of the gaseous distribution and results in stochastic asymmetries of the jets as one signature of this strong interaction. The resulting blast wave in a gas-rich galaxy compresses structures to high density where cooling is highly effective and impedes the cloud's pressure support and thereby its adiabatic re-expansion. In this paper, we extend our earlier study to include star formation. We will here focus on the impact of the jet on the star-forming gas in the galaxy and its observable signatures. We find that a strong increase in SFR is expected with a clear morphological signature in the stellar distribution. While the total number of stars in a given galaxy probably is not changed much by this, it would still be expected to be observable while it is ongoing and can have a significant impact on the galaxy's evolution.

The paper is organized as follows: in Section 2, we summarize the setup of the simulation and state the differences to the setup of Paper I. The results are given in Section 3, separating three different stages found in the simulation. The results are then discussed in Section 4.

2 THE MODEL

We model the host galaxy as a clumpy, disc-like distribution of gas with a log-normal probability distribution of the density (median $10 \, m_p \, \mathrm{cm}^{-3}$, mean $16.5 \, m_p \, \mathrm{cm}^{-3}$), an exponential radial profile with scale radius $R_0 = 5$ kpc and a sech^2 vertical profile with scale height $h_0 = 1.5$ kpc, reminiscent of a massive and thick galactic gaseous disc at high redshift (Genzel et al. 2006). The width of the log-normal density probability distribution corresponds to a turbulence of Mach number 5 ($\sim 80 \, \mathrm{km \, s}^{-1}$), which is similar to large evolving discs at high redshift (Förster Schreiber et al. 2009). The two-point structure of the density field is described by a Fourier spectrum that follows $E(k) \propto k^{-5/3}$ for large wave numbers k, but is damped towards smaller wave numbers to suppress inhomogeneities on scales larger than the disc scale height. The total mass of the disc is $1.5 \times 10^{11} \, \mathrm{M}_\odot$. The disc is embedded in a homogeneous hot atmosphere with a density of $0.05 \, m_p \, \mathrm{cm}^{-3}$ and a temperature of 1.15×10^7 K. The setup is almost identical to the one described in Paper I; differences are noted in this section. The jet is implemented as a cylindrical orifice of jet plasma (density $5 \times 10^{-5} \, m_p \, \mathrm{cm}^{-3}$, speed $0.8 \, c$) with the same pressure as the environment, a radius of $r_j = 0.4$ kpc and an initial length in both directions of $3r_j$, respectively.

We include radiative cooling by a tabulated cooling function for atomic processes down to 10^4 K as in Sutherland & Dopita (1993) with a metallicity $Z = 0.5 \, Z_\odot$ (Erb 2008), which is a very important effect in the disc due to the high densities and correspondingly short cooling times. No strong dependence on the metallicity or the exact form of the cooling function is expected since the mechanism found in our simulations can simply be understood by the fact that the cooling becomes more efficient (shorter cooling times) for denser gas. To avoid the need to include a fine-tuned feedback recipe to stabilize the cooling disc against the vertical gravity component, we exclude gravity in the simulations and stabilize the disc by imposing a minimum temperature of 10^4 K, which mimics a strong radiative heating from the stars that prevents any cooling below the threshold although this might still be expected in dense, shielded regions.

Since cooling is included, no truly static setup of the disc is possible and we run control simulations of the disc without the jet for
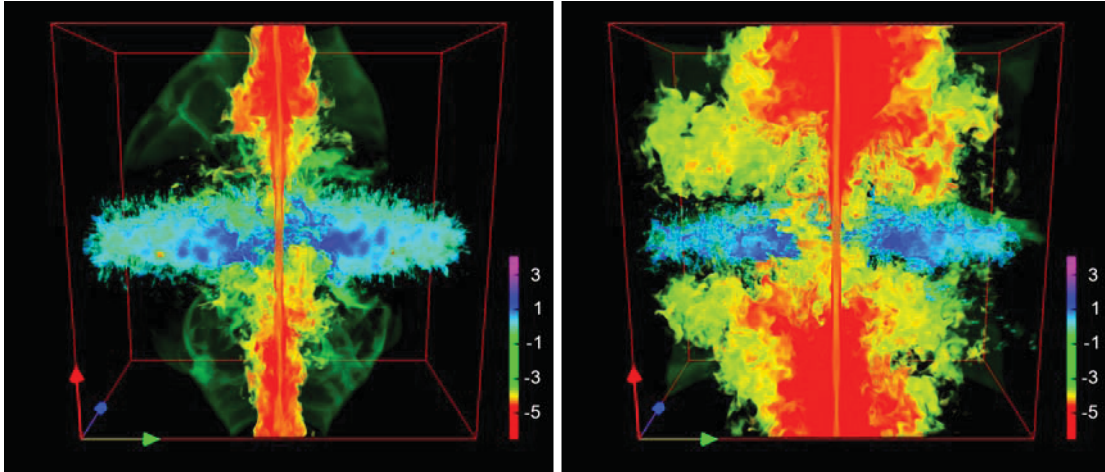
Figure 1. Density volume rendering of the central part of the domain (32 kpc box length) at $t = 14$ (left) and $t = 22$ Myr (right). Only the $z > 0$ half is shown and densities close to the ambient X-ray gas are transparent to give a tomographic view. The colour bars show log ρ in units of m_p cm^{-3}.

comparison in order to monitor the evolution of the undisturbed disc. In contrast to Paper I, we use constant pressure for the initial conditions of the entire domain, however, enforcing a pressure corresponding to a minimum temperature of $T_{min}/\mu = 10^4$ K where necessary (μ: mean particle mass in proton masses). Although the disc gas cools rapidly to T_{min} and drops out of pressure balance, it shows only little evolution in the fluid variables with little impact on the dynamics (however, resulting in a different jet asymmetry than in Paper I). To allow for a more relaxed disc state, the jet of power $L_{kin} = 5.5 \times 10^{45}$ erg s^{-1} is only started at $t = 10$ Myr. The simulations are carried out using the RAMSES 3.0 code (Teyssier 2002), a non-relativistic second-order Godunov-type shock-capturing adaptive mesh refinement code. The grid is refined to the maximum of 62.5 pc cell size in all regions of interest. For the many dense clumps, the cooling length cannot be resolved and hence shells formed by shocks are expected to be thinner and denser in nature for these cases. We include tracer fields for both the jet plasma and the cool disc gas to follow its spatial distribution independent of mixing processes. Magnetic fields are not considered in this study. Our earlier magnetohydrodynamic simulations (Gaibler et al. 2009) showed that for the morphology of the jet cocoon at large scales they play an important role since they efficiently suppress Kelvin–Helmholtz instabilities at the contact discontinuity. Although the interaction of the jet with individual clumps of gas may be affected by magnetic fields and reduce the efficiency of ablation, this is beyond the scope of this paper and we leave it to a future study.

In this study, we use a star formation model (Rasera & Teyssier 2006), where particles are generated in higher density regions of hydrogen number density $n_H > n_\star$ ($\rho > 1.31 \, m_p \, n_\star$) according to $\dot{\rho}_\star = \epsilon \rho / t_{ff}$, where t_{ff} is the local gas free-fall time and ϵ the star formation efficiency. This method is widely used in hydrodynamic simulations (e.g. Kravtsov 2003; Springel & Hernquist 2003; Dubois & Teyssier 2008; Schaye & Dalla Vecchia 2008), supported by observations (Krumholz & Tan 2007) and is able to recover the Kennicutt–Schmidt law (Kennicutt 1998) in simulations. After spawning a star particle, the corresponding gas is removed from the grid. We use two pairs of parameters ($n_\star = 0.1$ cm^{-3}, $\epsilon = 0.025$) and ($n_\star = 5$ cm^{-3}, $\epsilon = 0.05$) to check the impact of star formation being more strongly localized in high density regions. The efficiency parameters ϵ were chosen to get a SFR ~ 150 M$_\odot$ yr^{-1} similar to those observed in massive high-redshift galaxies (Genzel et al. 2010). The higher star formation threshold can be regarded as

being more realistic for our resolution, but shows more relaxation in the disc (which itself tends to decrease the SFR with time).

3 RESULTS

We here briefly summarize the formation of the blast wave as reported in Paper I. The jets produce a blast wave in the central region of the disc since the density contrast between the jet and the dense gas ($\eta = \rho_j/\rho_{disc}$) is very strong ($\eta < 10^{-5}$), causing the jet head to stall and deposit its energy in mostly thermal form into the disc gas. This is also true at later times, when the jet breaks out of the disc, but since the density contrast is weaker, a stronger forward propagation results. Figs 1 and 2 give an overview of the evolution of the jet–disc interaction (see also fig. 3 of Paper I and the supplementary movie there). Since the jet feedback is energy driven, the large mechanical advantage (Wagner & Bicknell 2011) allows a much stronger effect than expected for a momentum-driven jet feedback model (Krause & Gaibler 2010). The early evolution hence is dominated by the effects of the blast wave rather than direct interaction of the jet beam with the ISM clouds, but the dense clumps inhibit the propagation of the jet and thus help to deposit the jet energy closer to the centre of the galaxy, thereby feeding the blast wave.

The compression of gas by the blast wave and its short cooling times result in a considerable increase in the SFR despite the excavation in the centre (Fig. 3). The simulation with a higher star formation threshold ($n_\star = 5$ cm^{-3}) shows a much stronger increase in star formation than the one with a lower threshold (480 versus 280 M$_\odot$ yr^{-1} at $t = 22$ Myr). This can be understood as a consequence of the stronger cooling and compression at these potential sites of star formation. Also, the star formation is more concentrated towards the centre with the higher threshold due to the radial density profile. We have performed control simulations without the jets to ensure that the changes in star formation are actually caused by the jet activity, since the undisturbed disc cannot be in hydrostatic equilibrium due to the cooling. Indeed, the undisturbed disc evolves much more moderately than the disc with active jets. The relaxation effects in the disc are somewhat larger for the higher threshold run since stars are formed in smaller regions with higher densities, but they are generally opposite to the effects caused by the jet (they tend to lower the SFR). By the end of the simulation, the SFR is still increasing continuously. This can be understood by looking at the star formation in three different cylindrical regions around the disc
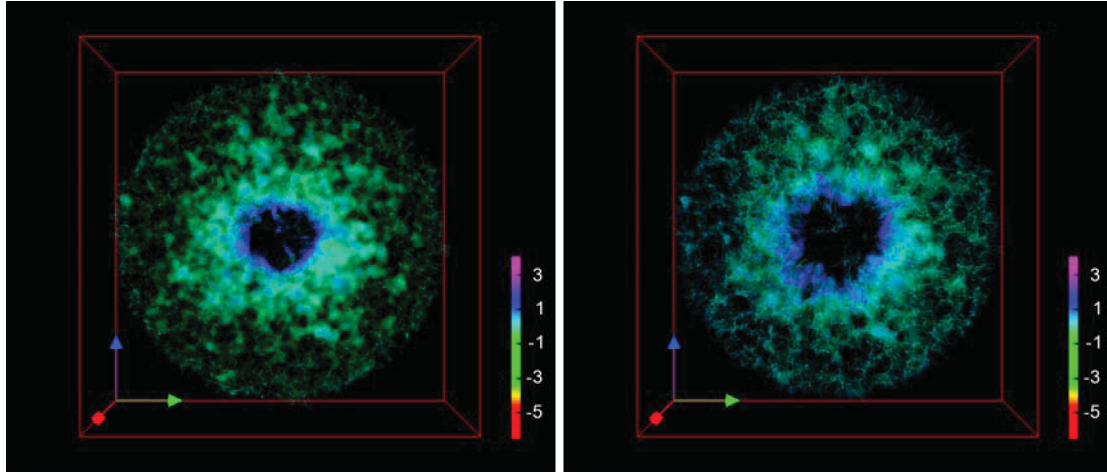
Figure 2. Density volume rendering of the high density gas in the disc (face-on view) at $t = 14$ (left) and $t = 22$ Myr (right). The box length is 32 kpc, lower density regions are transparent and the colour scale is the same as in Fig. 1.
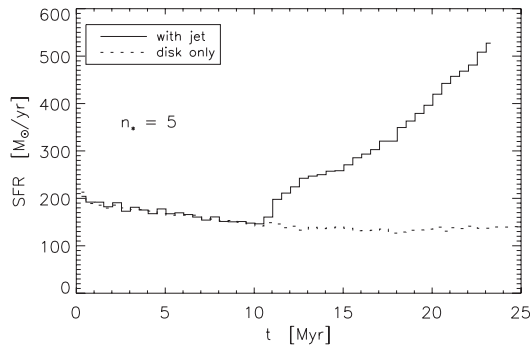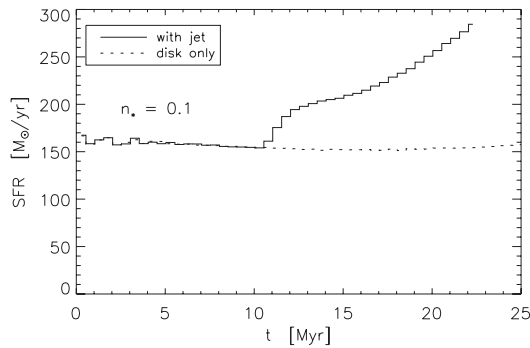

Figure 3. Total SFR for star formation thresholds of $n_\star = 0.1$ cm^{-3} (top) and $n_\star = 5$ cm^{-3} (bottom). The jet is started at $t = 10$ Myr.

Figure 4. Evolution of the SFR for three cylindrical regions of the disc: the central area ($R < 3$ kpc), a ring-like region (3 kpc $\leq R < 6$ kpc) and the outer disc (6 kpc $\leq R < 16$ kpc). The top panel is for a star formation threshold $n_\star = 0.1$ cm^{-3}; the bottom panel for $n_\star = 5$ cm^{-3}. Only stars with $\Delta x < 10$ kpc from the disc plane are considered; the disc-only simulation is shown by *blue, thin* lines, and the *red, thick* lines include the jet.

axis (Fig. 4). In addition, Fig. 5 shows face-on and edge-on maps of the stars at three different times.

The SFR in the inner region ($R < 3$ kpc) drops after an initial increase caused by compression and the subsequent removal of gas. In the intermediate region, between 3 and 6 kpc, the SFR increases strongly by a factor of 2.5 and 3.5 for the low and high threshold, respectively, and then settles to this value since the main interaction region for the jet is then outside the disc and the increased SFR only continues eating up the generated high-density gas. The outer region ($R \geq 6$ kpc) only shows an increasing SFR at $t \gtrsim 14$ Myr, but it continues to rise until the end of the simulation. The increase in SFR at large radii is generated by the overpressure in the jet's bow shock and cocoon, which is compressing the entire ISM of the disc
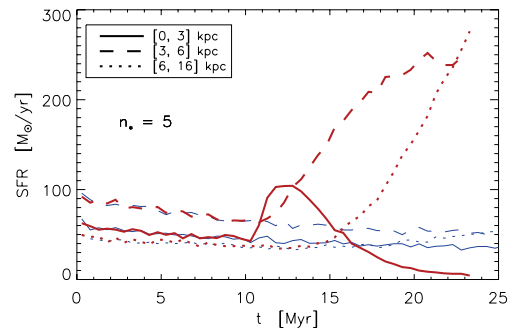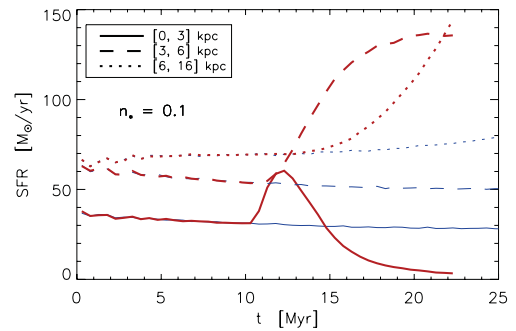
(Fig. 6), and thereby pushes its density beyond the star formation threshold. The control simulations show a slightly decreasing SFR except for the outer area, where it increases a bit since the ambient gas is already at slightly higher pressures than the cooling disc gas. So far, we cannot tell from the simulations how the long-term evolution of the SFR in the outer region is changed by the jet and how this depends on the modelling of the disc. Yet it is evident from the simulations that this pressurizing of the disc occurs and may result in a large number of stars being formed.

For the overall impact of the jet activity, we identify three phases that explain the evolution of star formation in the disc: (a) excavation
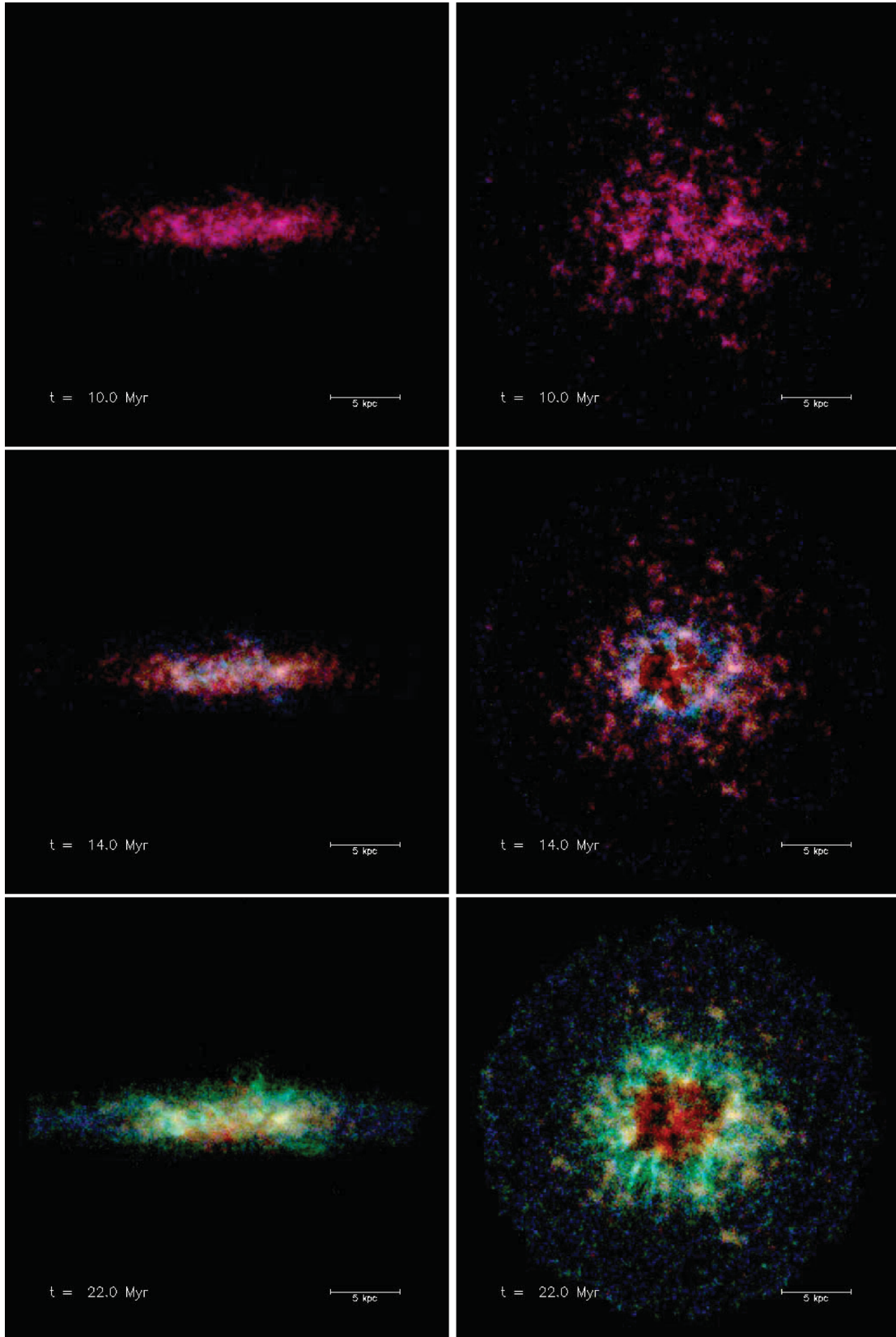
Figure 5. Star formation maps for $t = 10$ Myr (top), $t = 14$ Myr (middle) and $t = 22$ Myr (bottom row) as RGB composite (left: edge-on view, right: face-on view). Newly formed stars (formed within the last 1 Myr) are shown in blue, all other are shown either in red (stars formed at $t \leq 10$ Myr in the undisturbed disc) or green (stars formed at $t > 10$ Myr, jet was active). The images refer to the simulation with the high density threshold ($n_\star = 5\,\mathrm{cm}^{-3}$), a scale bar with 5 kpc length is given.
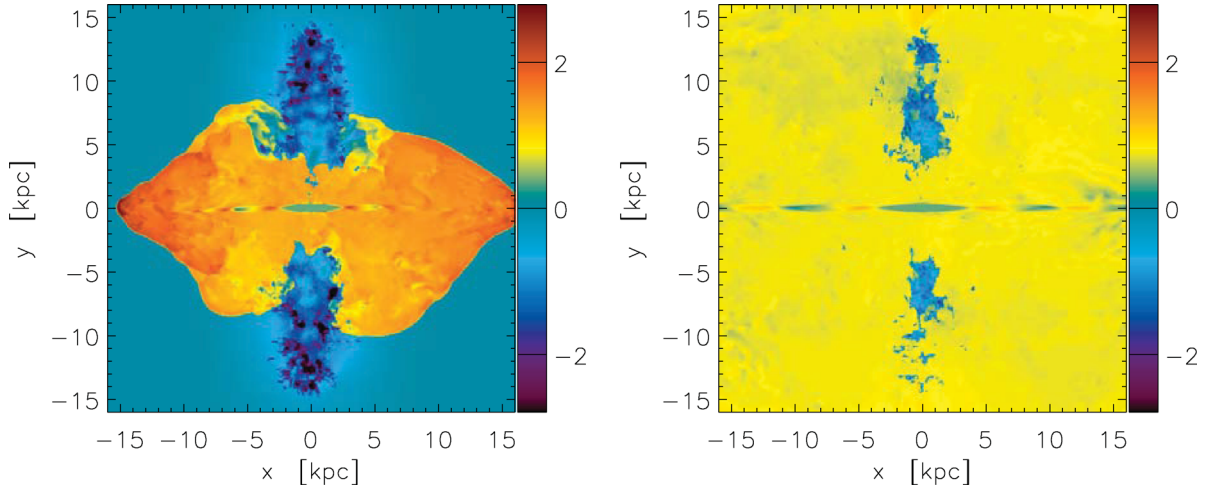
Figure 6. Pressure slices through $z = 0$ at $t = 13$ (left) and $t = 22$ Myr (right), showing $\log p$ normalized to the ambient pressure.

of a central cavity, (b) compression of disc gas and triggering of ring-like star formation by the blast wave and (c) late-time evolution of the disc in the jet cocoon. In the following subsections, we will address these phases in more detail. The phases should not be understood as consecutive phases, since they overlap temporally.

3.1 Phase A: formation of a central cavity

The most direct consequence of the blast wave is the formation of a cavity in the disc centre since the bow shock pushes intermediate density gas outwards. The expansion can be approximated by a spherical shape, and assuming a constant energy input by the jet, the blast wave evolution can then be described by the one given in Krause (2005), keeping in mind the expectable deviations due to the inhomogeneities in the disc. The blast wave expands until it leaves the disc vertically, and then venting its high pressure efficiently though this channel since the weaker density contrast there results in a faster jet propagation. Consequently, the lateral expansion of the cocoon into the disc slows down. As can be seen from the simulation, this breakout happens approximately when the bow shock reaches a radius of $r_{cav} \sim 2h_0$, where the vertical density profile dropped to 0.07 of the midplane density. The time needed for this is, according to the blast wave approximation,

$$t_{cav} \sim (2h_0)^{5/3} \left(\frac{5L_{kin}}{4\pi\rho} \right)^{-1/3}, \tag{1}$$

with $t_{cav} \approx 3$ Myr for our simulation parameters and applying the mean central disc density as ρ. This means that for thinner discs and lower densities, the time-scales can be much shorter than 1 Myr, with $r_{cav} \ll 1$ kpc.

The 'cavity' actually is not empty but still contains a considerable amount of gas (Fig. 7): about half the mass initially present in the centre is still there after the passage of the blast wave. However, the gas is located in very dense clumps and filaments with only a small filling factor.

We can furthermore estimate the energy deposited in this blast wave phase into the removal of gas by assuming that half the mass of this volume is accelerated to a speed of $v = 0.5\,r_{cav}/t_{cav}$. With $M \sim 16\pi h_0^3 \rho/3$, we get

$$E_{kin} \sim 0.3\,h_0^{5/3}\rho^{1/3}L_{kin}^{2/3}, \tag{2}$$

which in our case gives $\sim 5 \times 10^{58}$ erg. For comparison: the jet injects 5×10^{59} erg within $t_{cav} \approx 3$ Myr.
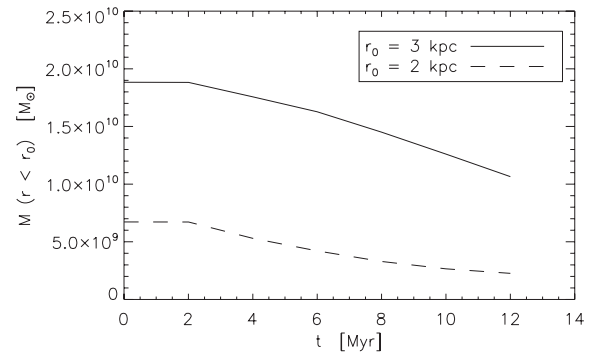

Figure 7. Evolution of the mass inside a spherical region $r < r_0$ around the centre with $r_0 = 2$ kpc and 3 kpc. Initially overwriting the jet nozzle region accounts for $5.4 \times 10^8\,\mathrm{M_\odot}$, and $<10^9\,\mathrm{M_\odot}$ over the entire run time.

In our simulation, we start with an initial jet length of already 1.2 kpc, so we actually have two blast waves originating from the tip of the jet beam, respectively. These blast waves meet near the disc midplane, get shocked by their respective counterparts and compress gas into a thin disc-like structure (easily visible in fig. 3 of Paper I), which is immediately destroyed by the shear flows in the cocoon and fragments into the filaments and clumps that remain located in the cavity. If the imposed initial jet length were zero, the two blast waves would be merged from the beginning as a single blast wave originating from the disc centre, skipping the intermediate creation of a dense, double-shocked cavity disc. We can now estimate what can be expected in nature for this early blast wave formation.

The blast wave behaviour is a result of the jets having a much lower density than the ambient gas ($\eta \ll 1$), where then momentum balance enforces a slow propagation and most of the energy is deposited in thermal energy. In contrast, high density jets ($\eta \gg 1$) show a ballistic propagation behaviour. Hence, the blast wave phase will begin once the jet density drops strongly below the local ambient gas (i.e. once it encounters a region of much higher density). Larger jet beam widths are observed at larger distances from the galactic nucleus, stable jets showing only small opening angles of a few degrees. As jets expand slowly, their density decreases $\propto r^{-2}$ with distance (however, note that a Lorentz factor $\gg 1$ on the pc scale increases the effective density of the jet). Correspondingly, the jet might become underdense already at the scale of 10 pc to

reach the strong density contrast we have at the kpc scale. These numbers are clearly very dependent on the jet properties and the gas distribution in the centre of the galaxy, but help putting this early stage into context. Once the two blast waves have merged, the evolution becomes independent of the initial blast wave locations. This consideration tells us that our setup is robust and despite the expected morphological differences at small scales, the results of this study would not be affected significantly.

Some disc gas gets expelled by the interaction with the jet, as can be determined by the compressible disc gas tracer field. A mass of the order of a few $10^8 \, M_\odot$ on each side (for $|x| > 10 \, \text{kpc}$) is moved outwards from the initial disc ($|x| < 4 \, \text{kpc}$) with an asymmetric distribution (2 versus $8 \times 10^8 \, M_\odot$), as expected for the asymmetric interaction with the disc gas. By $t = 24 \, \text{Myr}$, it extends out to $\approx 20 \, \text{kpc}$ above the disc plane. We note that the star formation at larger distances from the disc (more than 10 kpc above the disc plane) is ignored in our SFR – it is generally low ($10^7 \, M_\odot$ for $n_\star = 5 \, \text{cm}^{-3}$ during the entire simulation).

3.2 Phase B: ring-like star formation

While the blast wave creates a cavity in the disc centre, it pushes gas outwards and compresses the disc at the cavity boundary with a ring-like or hour-glass shape. While the bow shock in the vertical direction reaches out to lower densities, where the propagation becomes easier, it is much harder near the disc plane. The dense clumps in the disc with densities of $> 10 \, m_p \, \text{cm}^{-3}$ have cooling times of $\lesssim 100 \, \text{yr}$ at temperatures slightly above $T \sim T_{\text{min}}$. Once they get shocked by the blast wave, they are compressed but lose their pressure support almost instantly, which prevents later re-expansion (see also the simulations by Mellema, Kurk & Röttgering 2002; Fragile et al. 2004). This happens even after the bow shock has passed since the post-shock pressure is $\sim 10^3$ times higher than initially in the disc, causing the clumps to collapse further.

The bow shock does not propagate very far into the disc due to the large mass in the disc and since the lateral expansion stalls once the jet has broken through the disc vertically. The strong compression of gas at the cavity boundary, however, leads to very efficient star formation with a ring-like morphology. Although our physical understanding of star formation is still limited, it is clear that high gas densities and a strong increase in environmental pressure have a strong impact on the actual star formation processes in molecular clouds (Krumholz, Dekel & McKee 2012), which cannot be modelled within this simulation.

The strong increase in density can also be seen clearly in the filling factor of the dense gas (Fig. 8). Before the jet is launched, the filling factor for high-density gas decreases since this phase at $T = T_{\text{min}}$ has a higher pressure than the lower density gas and expands (this is the relaxation process). However, once the jet becomes active, the filling factor increases by approximately one order of magnitude. The largely increased mass in dense regions then results in much larger star formation.

The phase diagrams at three different times shown in Fig. 9 give a different view of the interaction of the jet with the dense and dilute disc phases. Two lines, indicating the path for adiabatic expansion and for constant pressure, are overplotted. Gas cooling to $T = T_{\text{min}}$ inevitably causes pressure gradients within the disc, resulting in the hot and the very dense phase of the ISM being at higher pressure than the intermediate density gas in the disc and consequently expanding during the early relaxation phase. Without additional heating processes (note that supernova feedback is not enough to balance the large radiative losses), no dynamical equilibrium can be
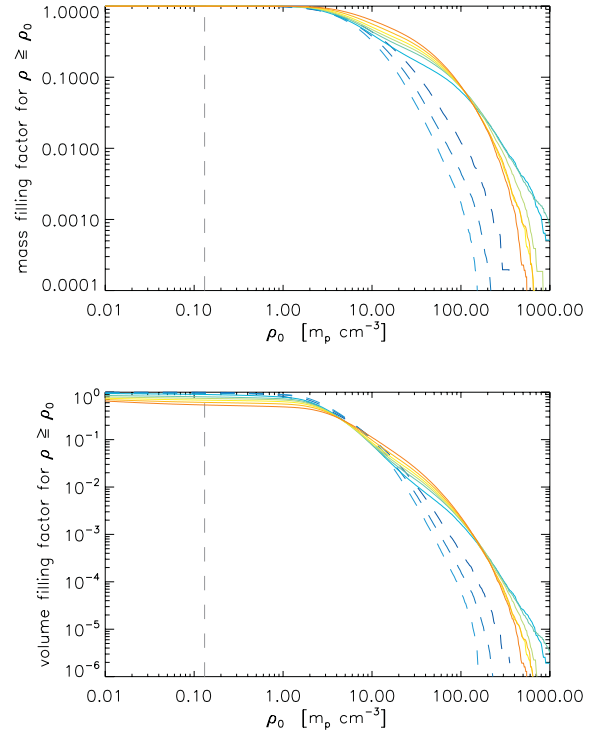

Figure 8. Evolution of the mass and volume filling factors of the disc. The time evolution is indicated by colour, going from blue via green and yellow to red. For early times (blue, dashed lines, $t = 0, 5$ and $10 \, \text{Myr}$), when the jet is still off, the filling factor at $\rho \gtrsim 10 \, m_p \, \text{cm}^{-3}$) decreases. With an active jet (solid lines, $t = 12, 14, 16, 18, 20$ and $22 \, \text{Myr}$), it quickly increases, but then decreases again for the highest densities. Please note the jump between $t = 10$ and $12 \, \text{Myr}$. The star formation threshold $n_\star = 0.1 \, \text{cm}^{-3}$ is indicated as the grey vertical line (dashed). The disc is defined as the geometrical region, where the disc density profile is larger than $\exp(-2) = 13.5$ per cent of its central value.

established to keep the disc stable. We have deliberately chosen to neglect these processes since we cannot model them in a physically correct way and our setup without gravity exhibits only weak relaxation during the simulated time. At $t = 10 \, \text{Myr}$, only little gas is left at intermediate temperatures. Once the jet is active ($t = 12 \, \text{Myr}$), the jet cocoon appears as a new region at higher pressures. It extends from high temperatures, overpressured with respect to the jet nozzle and the ambient gas, down to lower temperatures and high densities. The latter part is the interaction and mixing zone between the dense disc gas and the very low density jet plasma. Here, the cooling times are short and the gas cools down quickly. There is a clear accumulation of gas at $T/\mu \approx 10^5 \, \text{K}$ (where cooling times become somewhat larger) before it ends up quickly with $T = T_{\text{min}}$ and underpressured, then reaching up to higher densities. At $t = 20 \, \text{Myr}$, the cocoon is less overpressured and visible as a distinct $p = \text{const}$ feature. Now the interaction with the ambient gas is more prominent and the gas distribution forms a downward-bent cooling path, which supplies the disc with an increased amount of dense, star-forming gas.

3.3 Phase C: later evolution in the jet cocoon

At later times, when the jet mostly interacts with the ambient gas, the changed environment of the gas disc becomes important: the bow shock now encloses the entire disc and the increased pressure of the jet cocoon affects the disc. This is due to both the ram pressure of the
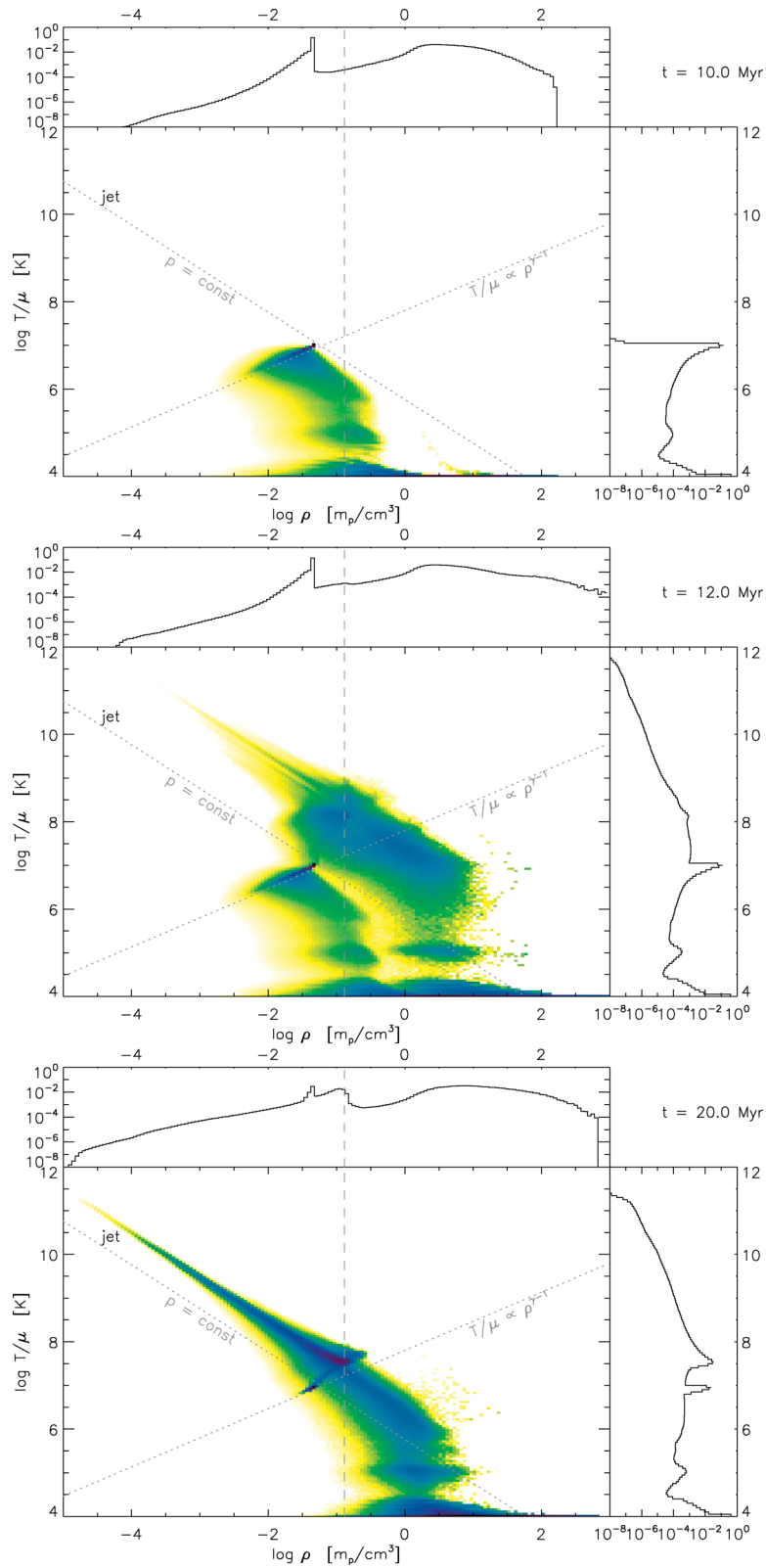
Figure 9. Phase diagram for the cells in the central $(32\,\mathrm{kpc})^3$ box, which enclosed the entire disc: temperature T/μ versus density ρ for three different times (the jet starts at $t = 10\,\mathrm{Myr}$). For comparison, lines of constant pressure as well as adiabatic expansion/compression ($T \propto \rho^{\gamma-1}$) are overplotted (dotted), the star formation threshold $n_\star = 0.1\,\mathrm{cm}^{-3}$ is shown as a vertical line (dashed) and the location of the jet nozzle is indicated. Mass-weighted density and temperature histograms with logarithmic bins are attached to the phase diagram, respectively.
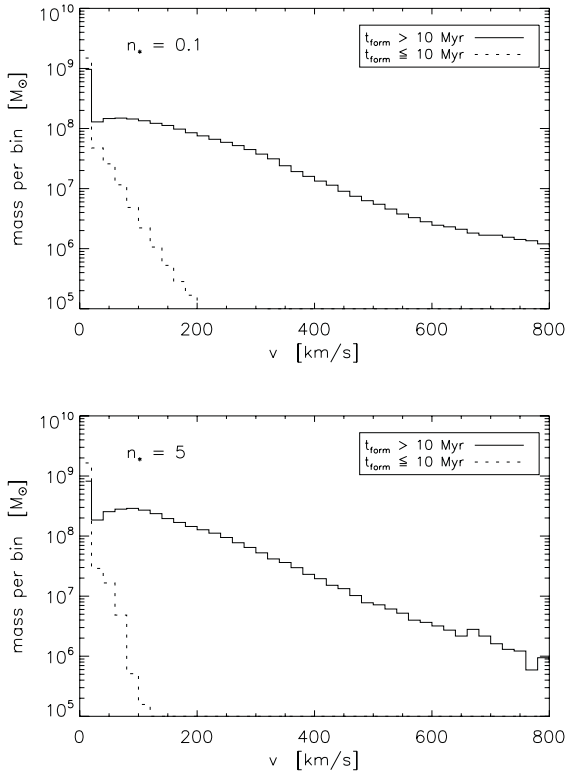
Figure 10. Velocity distribution of the stars at $t = 22\,\mathrm{Myr}$ for the low ($n_\star = 0.1\,\mathrm{cm}^{-3}$, top) and high ($n_\star = 5\,\mathrm{cm}^{-3}$, bottom) star formation threshold. The contributions are shown separately for stars formed before (dotted) and after (solid) the jet starts at $t = 10\,\mathrm{Myr}$. The histograms show the mass of the stars within a bin size of $20\,\mathrm{km\,s}^{-1}$.

backflow with its vortices and the thermal pressure of the cocoon. Since the cocoon turbulence is in the subsonic or transonic regime, the thermal pressure dominates somewhat over the ram pressure. The cocoon pressure now sets the environmental pressure for the gas disc, which gets compressed. In our simulation, this is mostly on the surface of the disc, but with time this pressure will affect the entire disc. There is also ablation at the disc surface by the cocoon plasma; however, this is mostly intermediate density gas – the high density, star-forming gas is much more robust and harder to affect, and at sub-resolution scales it would also be stabilized by the self-gravity of the cloud.

Because the cocoon pressure drops as the radio source expands, the disc compression effect will eventually come to an end. Gaibler et al. (2009) find that jet cocoons are no longer strongly overpressured once the source extends over more than $\sim$100 kpc, where self-similar expansion then breaks down. We expect disc compression to be effective over approximately the active phase of the source or a bit longer. The total stellar mass formed by phase C is comparable to that of the previously described phase B.

3.4 Stellar velocities

The dense gas is not only compressed by the blast wave and forms stars – it is also accelerated by the ram pressure, mostly in the radial direction. This motion is imprinted on the newly formed stars within the clumps, which thus can show rather high radial velocities (Fig. 10) of several $100\,\mathrm{km\,s}^{-1}$, even exceeding the escape velocity of the galaxy. The disc-only simulations, in contrast, show much lower velocities caused by the gas motions. This higher velocity dispersion may actually be an observable signature of these stars.

While we expect this to occur also in nature, we caution that the present simulations are not sufficient for the determination of credible velocities because of two important points: first, the stars are not decelerated by gravitational forces since gravity is neglected in the setup, which is acceptable for the hydrodynamics on the short time-scales considered but has considerable impact on the stellar velocities. Second and even more important, stars form in the cores of molecular clouds at densities rather higher than the ones resolved here. Hence, the real velocities of these cores are considerably lower than for the gas at densities corresponding to the star formation threshold $n_\star$. This is expected to depend on the internal structure of the clouds and the efficiency of momentum transfer. Accordingly, the measured velocities are upper limits. We note, however, that the velocity distributions for the two star formation thresholds considered are not drastically different. About 8.6 ($n_\star = 0.1\,\mathrm{cm}^{-3}$) or 8.3 per cent ($n_\star = 5\,\mathrm{cm}^{-3}$) of the stars (2–3 $\times 10^8\,\mathrm{M}_\odot$ in absolute numbers) formed at $t \geq 10\,\mathrm{Myr}$ have velocities of $\geq 300\,\mathrm{km\,s}^{-1}$. Follow-up simulations with gravity and much larger resolution for the gas clouds will be needed to assess this aspect quantitatively.

4 DISCUSSION

4.1 Consequences for galaxy evolution

With the present simulations, we examine the impact of jets on a massive disc-like galaxy. The properties of the gaseous disc were chosen to be comparable with (non-merger) massive star-forming galaxies observed at redshifts of $z > 1$. The onset of the jets lead to an increase in SFR by a factor of 2 and more. During 12 Myr of jet activity, an additional stellar mass of $1.6 \times 10^9\,\mathrm{M}_\odot$ ($7.2 \times 10^8\,\mathrm{M}_\odot$) is formed for our runs with a star formation threshold of $n_\star = 5\,\mathrm{cm}^{-3}$ ($0.1\,\mathrm{cm}^{-3}$), respectively, compared to the quiescent disc simulation. Since the simulations are covering only $\sim$12 Myr of jet activity, it is still difficult to estimate the long-term effects on the galaxy. As for the generally assumed negative feedback from jets, we have found that the reduction of star formation occurs mostly in the central region of the disc and is much smaller than the enhancement of star formation in the rest of the galaxy. By the end of the simulation, the SFR at intermediate radii does not increase further and would decrease slowly as the densest clumps are converted into stars. At larger radii, the SFR is still continuously increasing and is expected to stay at a high level until the jet cocoon pressure has dropped to a value near the original ambient pressure (cf. Gaibler et al. 2009), which happens after a few $10^7\,\mathrm{yr}$. Altogether, the total stellar mass generated additionally by the jet activity may be up to $\sim 10^{10}\,\mathrm{M}_\odot$. While this is only a fraction of the total stars formed considering the high quiescent (disc-only) SFR, these stars are distributed non-uniformly throughout the disc and are of similar age.

Both SFR-enhancing phases (B and C) are caused by the large amount of thermal energy generated by the jet as it forces its way though the ISM. Although direct interaction of the jet beam with clouds is limited to a small volume, the resulting pressure affects a fair fraction of the disc at the early stage and eventually all of the galaxy once the bow shock has reached beyond the galaxy's radial extent. By that time (in our simulation within $\sim$10 Myr), the galaxy is embedded in a hot and low-density atmosphere (the jet cocoon) with a pressure about one order of magnitude larger than initially. It is quite evident that increasing pressure in and around a galaxy within a relatively short time will have a considerable effect on its star formation, causing higher densities and higher SFRs eventually – independent of whether SFRs are understood in terms of the local free-fall time (as done by the code), the Kennicutt–Schmidt law

(Kennicutt 1998) or a global dependence on pressure (Wong & Blitz 2002; Blitz & Rosolowsky 2004).

Wagner & Bicknell (2011) note that the ablation time-scale in general would be shorter than the cloud collapse time-scale due to the large velocities in the jet cocoon, and destruction of the clouds hence would be expected without any possibly associated star formation. However, while ablation may actually remove a considerable fraction of the dense clouds, we expect that only the cloud envelopes with their lower densities would be affected. The star formation takes place only in the highest density regions where, at densities of $\sim 10^4$ cm^{-3} and considering stabilization by self-gravity, the jet will hardly have a totally destructive effect, in the worst case leaving a naked high-density core. Shocks driven into the clouds will be strongly radiative and dense shells formed by that would additionally protect the core even though the cloud may fragment (cf. Mellema et al. 2002; Cooper et al. 2009). Since the environmental pressure of the cloud jumps to very large values, the cloud core will eventually be compressed to a higher density with an anticipated increase in star formation there. This might even happen in the cleared-out central disc region, where naked molecular cloud cores could be left embedded in the jet cocoon. This can be further quantified by the time-scales of the processes competing with the cloud collapse. Following Cooper et al. (2009) and using the data from the simulation and a fiducial radiative cloud of $100 m_{\rm p}$ cm^{-3} and 100 pc radius, the cloud crushing time is $\gtrsim 10^8$ yr and the growth time-scale for Kelvin–Helmholtz instabilities is 10^5–10^6 yr. These are considerably larger than the cooling time for the dense clouds, and the Kelvin–Helmholtz time-scale would even be larger if magnetic fields were present in the clouds. Hence, the cloud would be stable against ablation until self-gravity takes over with a free-fall time-scale of ~ 3 Myr and subsequent star formation would be expected.

If star-forming molecular clouds are seen as transient objects generated within a dynamic ISM of different phases, one could argue that destruction of warm (intermediate density) gas by the jet as in the cloud envelopes cuts off the supply necessary for the formation of molecular clouds and thereby would lower the SFR on longer time-scales. In the present simulations, however, the amount of strongly cooling gas is not changed much by the jet activity: depending on the selection threshold, it decreases only by 3 per cent for gas with cooling times $\tau_{\rm c} < 10^5$ yr or even increases by 10 per cent for $\tau_{\rm c} < 10^3$ yr between $t = 10$ and 20 Myr, hence providing a reservoir for molecular cloud formation also after the jet activity has ceased.

We have performed the simulation with two different star formation thresholds ($n_\star = 0.1$ and 5 cm^{-3}) to examine resolution effects that are clearly expected for a setup with strong cooling. For both thresholds, the local Jeans length is resolved by ≥ 20 cells, and it could even be raised to 100 cm^{-3} for four cells per Jeans length. A stronger increase in SFR is found for the higher threshold, where star formation is more concentrated to the densest regions of the clouds, which we expect to be more realistic. Furthermore, the change in the density probability distribution function (PDF) caused by the onset of the jet activity is a robust and purely hydrodynamical result (cf. compressional forcing, Federrath et al. 2010) with the direct consequence of a larger expected SFR independent of the actual implementation; the time evolution of the PDF is much larger than the differences between the runs with different thresholds at equal times. This increase in the density PDF at high densities is also found in the simulations by Wagner & Bicknell (2011, private communication), with some differences due to the different setup. We are hence confident that the results are robust, and the enhancement

of star formation effects might even be stronger if self-gravity of the gas clouds were considered.

Thermal or kinetic AGN feedback in cosmological and galaxy evolution simulations (modelling radio and/or quasar mode) is often thought to heat or expel gas from the galaxy and to be acting mostly on the circum-galactic gas (e.g. Springel, Di Matteo & Hernquist 2005; Croton et al. 2006; Sijacki et al. 2007; Bower, McCarthy & Benson 2008; Booth & Schaye 2009; Dubois et al. 2012), lowering the SFRs. Our setup, in contrast, has shown the entirely opposite effect: the formation of an additional population of stars. The need for an additional boost of star formation has been recently suggested by Khochfar & Silk (2011). They argue that to recover the high specific SFRs that are observed in galaxies at $z > 5$, ΛCDM models need to introduce stochastic boosts in star formation. Such boosts could indeed be triggered by jet activity as presented here in gas-rich galaxies at $z > 5$. The main reason for the difference between our results and common AGN feedback simulations lies in the different treatment of the ISM and the collimated jets: whether it forms a rather continuous gas distribution or individual small-scale clouds are resolved and interact with the propagating jets. While on the AGN activity time-scale, our simulation shows a considerable positive feedback, this does not yet imply that there could be no negative feedback associated with jets: first, it is important to keep in mind that outside the galaxy, in the rather uniformly distributed and diffuse circum-galactic or intra-cluster gas, the feedback is still negative, heating the gas and quenching cooling flows. Secondly, on the galaxy scale, the formation of $\sim 10^{10}$ M$_\odot$ of stars (almost instantaneous compared to galaxy evolution time-scales and concentrated in certain regions, cf. Fig. 5) will eventually be joined by the stellar feedback from these stars. This may have a strongly negative effect on the later evolution of star formation. For smaller gas masses, the positive effect might be very small and more efficient ablation might cause negative feedback to be dominant for the lower-density environment, potentially resulting in positive feedback in gas-rich (high-z) and negative feedback in gas-poor (low-z) environments. We note that while this study addresses the physics of ongoing jet feedback, it is still unclear under which circumstances AGN jets are launched and how frequently jet activity would occur in gas-rich galaxies.

Clearly the present simulations do not include all physics that might be relevant; magnetic fields and cosmic rays might play a role, and small-scale shocks or turbulent mixing layers may be effective below the finite resolution of our hydrodynamical simulation. However, these effects would affect discs without jets in a similar way unless the star formation mechanism is particularly sensitive to the changes. Assuming that giant molecular clouds are essentially self-regulated inside (e.g. Krumholz, McKee & Tumlinson 2009), it is at least not obvious why the molecular cloud processes in the core would change drastically, except that the hydrodynamical interaction with their environment changes the global cloud properties. In our simulations, compression by the blastwave and the jet cocoon in general is the dominant effect, with ablation and stirring of the cold clouds being limited to the surface of the disc. The long-term evolution of the galaxy and an exploration of the parameter space are beyond the scope of this paper and should be addressed in future studies.

4.2 Comparison to observations

As noted in Section 1, the observational evidence for positive feedback or jet-induced star formation is still limited, while the scenario in the light of the presented simulations appears almost inevitable from a theoretical point of view. Clearly, gas masses and jet

powers in the local Universe vary over a large range and the present study only probes one point in a large parameter space (powerful jets in massive high-redshift gaseous discs). Accordingly, the star formation induced by the jets in the often quite different nearby objects will be on a considerably smaller level and possibly be unrecognized. We have seen in the simulation that the jet causes a morphological disturbance in the stellar distribution – a ring or disc of stars is generated by the early blast wave of the jet expanding in the galaxy. Since the expansion becomes much slower and stalls once the jet is able to break out vertically through the dense gas, the radius of this stellar population should be of the order of a few vertical scale heights of the gas. For galaxies in the local Universe, this would be at some 100 pc. Interestingly, Jackson, Tadhunter & Sparks (1998) found a ring of young stars around the centre of Cygnus A, the most powerful radio source at low redshift ($z = 0.056$). They argue that the blue condensations are almost certainly due to young stars and not caused by scattering of the obscured quasar; the continuum energy distribution can be modelled by starburst activity much less than 1 Gyr ago, possibly an instantaneous burst with $t \leq 10$ Myr, which is compatible with the radio source age of $\sim 10^7$ yr (Krause 2005). Privon et al. (2012) derive an overall SFR of 10–70 $M_\odot$ yr^{-1} for Cygnus A. The morphology of the young stars is strikingly similar to the one found in our simulations. The radius of the stellar ring of ~ 2 kpc would mean that the ISM is rather extended in the vertical direction, but there are currently no observations available constraining the details of the distribution of a dense gaseous component.

Despite the small number of examples, the action of positive feedback is well compatible with or even supported by a number of observations mentioned in Section 1. In particular, the recent star formation activity in more than 75 per cent of small (<15 kpc) radio galaxies (Dicken et al. 2012) or the young stellar populations found in radio galaxies (Tadhunter et al. 2002; Wills et al. 2002; Holt et al. 2007; Baldi & Capetti 2008; Tadhunter et al. 2011) and the centres of radio galaxies (Aretxaga et al. 2001) may very well be caused by jet-induced feedback. And although the young stellar populations are mostly discussed in the context of merger-induced jet activity, it is not clear whether the merger scenario is a viable scenario and could explain the observations satisfactorily, whether it can be distinguished against jet-induced star formation and what effect jet activity would have while a merger is ongoing. The mere fact that the merger, increased star formation and radio jets occur at similar times does not give a causal relation, in particular since the duration of a single jet activity cycle is of the order of or even below the age accuracy of the young stellar population.

The additional stars in our simulation that have been formed due to the action of the jet are almost entirely located within the gaseous galactic disc. This may however not be interpreted as evidence against the possible jet-induced star formation away from the disc, aligned with the axis of the radio jet (e.g. McCarthy et al. 1987; Dey et al. 1997). This possible mode of star formation is associated with tens of kpc sized emission line haloes (e.g. Meisenheimer & Hippelein 1992; McCarthy 1993; Best, Longair & Röttgering 1997; Miley & De Breuck 2008), which are quite possibly due to gas extracted from the galaxy (Nesvadba et al. 2008; Krause & Gaibler 2010). In our simulation, we find that approximately 10^9 $M_\odot$ of disc gas leaves the galaxy during the time the jet is active, though this gas does not remain dense enough to form the observed emission line gas. The absolute number is rather encouraging, and should be regarded as a lower limit, since we neglect several important effects in this regard in our simulations: first, we do not simulate the initial phase of the jet until it reaches the extent of 1 kpc. This phase might

result in substantial outward motions of the gas (Wagner & Bicknell 2011). Secondly, the ISM is expected to be turbulent, which might also help to get it started from the disc. Thirdly, the enhanced supernova feedback due to the jet-induced star formation within the disc should also add a considerable amount of kinetic energy to the gas. Once having left the disc, the gas would be further stirred up by interaction with the turbulent jet cocoon (Krause & Alexander 2007). Also magnetic fields (neglected in our simulation) might help to stabilize the emission line phase. Finally, while generally speaking, we simulate a high power (FR II, Fanaroff & Riley 1974), the jet power in our simulation is set rather conservatively. If we would increase it by a factor of 10, and if the amount of ejected mass would scale linearly with the jet power, we would reach the right order of magnitude that has been claimed by the observations (Nesvadba et al. 2008). Since there is not even gas cold enough to form emission line regions present in our simulations outside the galactic disc, which is however clearly present in nature, it is evident that our simulations do not address jet-induced star formation outside the galactic disc.

Our simulations include a high-power FR II jet – a case which is quite rare in the local Universe. The low-power (FR I) jets are much more abundant and evolve differently. Yet, the early stage may be very similar since FR I jets are still relativistic at small scales and would deposit their mechanical power into the ISM in a similar way as for the simulated case. Since their luminosities are much lower, their effect on the dense gaseous phase might be much smaller and restricted rather to small radii, which is possibly difficult to detect. In general, low-redshift radio galaxies show low SFRs as derived from polycyclic aromatic hydrocarbon (PAH) emission features (Shi et al. 2007; Ogle et al. 2010), even though some of them have fairly large masses of molecular gas. Yet, we believe that a careful examination of radio galaxies for a central star formation and a global enhancement of star formation once the bow shock has propagated beyond the galaxy should be done, including formation of molecular gas at these locations, in order to shed more light on the impact of jet activity on the evolution of their host galaxies. Observations at high redshift are clearly more demanding. Stacey et al. (2010) detected 158 µm [C II] line emission in galaxies at $z \sim 1$–2, and inferred most of the far-infrared and [C II] emission originates from kpc-scale cores in the AGN-dominated galaxies where the local far-UV field is much higher than in the star-formation-dominated galaxies. This led them to assert that the onset of AGN activity stimulates large-scale star formation, an argument also consistent with the detection of strong 88 µm [O III] and 122 µm [N II] emission in composite starburst AGN (Ferkinhoff et al. 2010, 2011). Seymour et al. (2008) were able to detect the PAH signature of a large SFR in a high-redshift radio galaxy. The wide range of observational results found for radio galaxies sources might indicate that positive feedback depends on certain conditions, and possibly be more effective for large disc masses which are more often found at higher redshift.

ACKNOWLEDGMENTS

REFERENCES

Antonuccio-Delogu V., Silk J., 2008, MNRAS, 389, 1750
Aretxaga I., Terlevich E., Terlevich R. J., Cotter G., Díaz Á. I., 2001, MNRAS, 325, 636
Baldi R. D., Capetti A., 2008, A&A, 489, 989
Best P. N., Longair M. S., Röttgering H. J. A., 1997, MNRAS, 292, 758
Best P. N., Kauffmann G., Heckman T. M., Brinchmann J., Charlot S., Ivezić Ž., White S. D. M., 2005, MNRAS, 362, 25
Bicknell G. V., Sutherland R. S., van Breugel W. J. M., Dopita M. A., Dey A., Miley G. K., 2000, ApJ, 540, 678
Bîrzan L., Rafferty D. A., McNamara B. R., Wise M. W., Nulsen P. E. J., 2004, ApJ, 607, 800
Blandford R. D., Rees M. J., 1974, MNRAS, 169, 395
Blitz L., Rosolowsky E., 2004, ApJ, 612, L29
Booth C. M., Schaye J., 2009, MNRAS, 398, 53
Bower R. G., Benson A. J., Malbon R., Helly J. C., Frenk C. S., Baugh C. M., Cole S., Lacey C. G., 2006, MNRAS, 370, 645
Bower R. G., McCarthy I. G., Benson A. J., 2008, MNRAS, 390, 1399
Chambers K. C., Miley G. K., van Breugel W., 1987, Nat, 329, 604
Clyne J., Rast M., 2005, Proc. SPIE, 5669, 284
Clyne J., Mininni P., Norton A., Rast M., 2007, New J. Phys., 9, 301
Cooper J. L., Bicknell G. V., Sutherland R. S., Bland-Hawthorn J., 2009, ApJ, 703, 330
Croft S. et al., 2006, ApJ, 647, 1040
Croton D. J. et al., 2006, MNRAS, 365, 11
de Avillez M. A., Breitschwerdt D., 2005, A&A, 436, 585
Dey A., van Breugel W., Vacca W. D., Antonucci R., 1997, ApJ, 490, 698
Dicken D. et al., 2012, ApJ, 745, 172
Dubois Y., Teyssier R., 2008, A&A, 477, 79
Dubois Y., Devriendt J., Slyz A., Teyssier R., 2012, MNRAS, 420, 2662
Dunn R. J. H., Fabian A. C., Taylor G. B., 2005, MNRAS, 364, 1343
Emonts B. H. C. et al., 2011, ApJ, 734, L25
Erb D. K., 2008, ApJ, 674, 151
Fanaroff B. L., Riley J. M., 1974, MNRAS, 167, 31
Federrath C., Roman-Duval J., Klessen R. S., Schmidt W., Mac Low M. M., 2010, A&A, 512, A81
Ferkinhoff C., Hailey-Dunsheath S., Nikola T., Parshley S. C., Stacey G. J., Benford D. J., Staguhn J. G., 2010, ApJ, 714, L147
Ferkinhoff C. et al., 2011, ApJ, 740, L29
Ferland G. J., Fabian A. C., Hatch N. A., Johnstone R. M., Porter R. L., van Hoof P. A. M., Williams R. J. R., 2008, MNRAS, 386, L72
Ferland G. J., Fabian A. C., Hatch N. A., Johnstone R. M., Porter R. L., van Hoof P. A. M., Williams R. J. R., 2009, MNRAS, 392, 1475
Förster Schreiber N. M. et al., 2009, ApJ, 706, 1364
Fragile P. C., Murray S. D., Anninos P., van Breugel W., 2004, ApJ, 604, 74
Gaibler V., Krause M., Camenzind M., 2009, MNRAS, 400, 1785
Gaibler V., Khochfar S., Krause M., 2011, MNRAS, 411, 155 (Paper I)
Genzel R. et al., 2006, Nat, 442, 786
Genzel R. et al., 2010, MNRAS, 407, 2091
Guillard P., Boulanger F., Pineau Des Forêts G., Appleton P. N., 2009, A&A, 502, 515
Holt J., Tadhunter C. N., González Delgado R. M., Inskip K. J., Rodriguez Zaurin J., Emonts B. H. C., Morganti R., Wills K. A., 2007, MNRAS, 381, 611
Hopkins P. F., Hernquist L., Cox T. J., Di Matteo T., Robertson B., Springel V., 2006, ApJS, 163, 1
Inskip K. J., Villar-Martín M., Tadhunter C. N., Morganti R., Holt J., Dicken D., 2008, MNRAS, 386, 1797
Jackson N., Tadhunter C., Sparks W. B., 1998, MNRAS, 301, 131

Kennicutt R. C., 1998, ApJ, 498, 541
Khochfar S., Silk J., 2011, MNRAS, 410, L42
Klamer I. J., Ekers R. D., Sadler E. M., Hunstead R. W., 2004, ApJ, 612, L97
Krause M., 2005, A&A, 431, 45
Krause M., Alexander P., 2007, MNRAS, 376, 465
Krause M. G. H., Gaibler V., 2010, in Antonuccio-Delogu V., Silk J., eds, Cambridge Contemporary Astrophysics, AGN Feedback in Galaxy Formation. Cambridge University Press, New York, p. 183
Kravtsov A. V., 2003, ApJ, 590, L1
Krumholz M. R., Tan J. C., 2007, ApJ, 654, 304
Krumholz M. R., McKee C. F., Tumlinson J., 2009, ApJ, 699, 850
Krumholz M. R., Dekel A., McKee C. F., 2012, ApJ, 745, 69
McCarthy P. J., 1993, ARA&A, 31, 639
McCarthy P. J., van Breugel W., Spinrad H., Djorgovski S., 1987, ApJ, 321, L29
McCarthy P. J., van Breugel W., Kapahi V. K., 1991, ApJ, 371, 478
Meisenheimer K., Hippelein H., 1992, A&A, 264, 455
Mellema G., Kurk J. D., Röttgering H. J. A., 2002, A&A, 395, L13
Miley G., De Breuck C., 2008, A&A Rev., 15, 67
Morganti R., 2010, in Antonuccio-Delogu V., Silk J., eds, Cambridge Contemporary Astrophysics, AGN Feedback in Galaxy Formation. Cambridge University Press, New York, p. 63
Mould J. R. et al., 2000, ApJ, 536, 266
Nesvadba N. P. H., Lehnert M. D., De Breuck C., Gilbert A. M., van Breugel W., 2008, A&A, 491, 407
Nesvadba N. P. H. et al., 2010, A&A, 521, A65
Nesvadba N. P. H., Boulanger F., Lehnert M. D., Guillard P., Salome P., 2011, A&A, 536, L5
O'Neill S. M., Jones T. W., 2010, ApJ, 710, 180
Ogle P., Antonucci R., Appleton P. N., Whysong D., 2007, ApJ, 668, 699
Ogle P., Boulanger F., Guillard P., Evans D. A., Antonucci R., Appleton P. N., Nesvadba N., Leipski C., 2010, ApJ, 724, 1193
Papadopoulos P. P., van der Werf P., Isaak K., Xilouris E. M., 2010, ApJ, 715, 775
Privon G. C., Baum S. A., O'Dea C. P., Gallimore J., Noel-Storr J., Axon D. J., Robinson A., 2012, ApJ, 747, 46
Rafferty D. A., McNamara B. R., Nulsen P. E. J., Wise M. W., 2006, ApJ, 652, 216
Rasera Y., Teyssier R., 2006, A&A, 445, 1
Schawinski K. et al., 2006, Nat, 442, 888
Schaye J., Dalla Vecchia C., 2008, MNRAS, 383, 1210
Scheuer P. A. G., 1974, MNRAS, 166, 513
Seymour N. et al., 2008, ApJ, 681, L1
Shi Y. et al., 2007, ApJ, 669, 841
Sijacki D., Springel V., di Matteo T., Hernquist L., 2007, MNRAS, 380, 877
Silk J., 2005, MNRAS, 364, 1337
Springel V., Hernquist L., 2003, MNRAS, 339, 289
Springel V., Di Matteo T., Hernquist L., 2005, MNRAS, 361, 776
Stacey G. J., Hailey-Dunsheath S., Ferkinhoff C., Nikola T., Parshley S. C., Benford D. J., Staguhn J. G., Fiolet N., 2010, ApJ, 724, 957
Sutherland R. S., Bicknell G. V., 2007, ApJS, 173, 37
Sutherland R. S., Dopita M. A., 1993, ApJS, 88, 253
Tadhunter C., Dickson R., Morganti R., Robinson T. G., Wills K., Villar-Martin M., Hughes M., 2002, MNRAS, 330, 977
Tadhunter C. et al., 2011, MNRAS, 412, 960
Teyssier R., 2002, A&A, 385, 337
Tortora C., Antonuccio-Delogu V., Kaviraj S., Silk J., Romeo A. D., Becciani U., 2009, MNRAS, 396, 61
Wagner A. Y., Bicknell G. V., 2011, ApJ, 728, 29
Wills K. A., Tadhunter C. N., Robinson T. G., Morganti R., 2002, MNRAS, 333, 211
Wong T., Blitz L., 2002, ApJ, 569, 157
Zanni C., Murante G., Bodo G., Massaglia S., Rossi P., Ferrari A., 2005, A&A, 429, 399

This paper has been typeset from a TEX/LATEX file prepared by the author.